ACS OMEGA

Article

Cite This: ACS Omega 2019, 4, 9065−9073

http://pubs.acs.org/journal/acsodf

Investigation of the Segregation of Binary Mixtures with Iron-Based Particles in a Bubbling Fluidized Bed

Sandra Turrado, José Ramón Fernández,* and Juan Carlos Abanades

Spanish Research Council, INCAR-CSIC, CO_2 Capture Group, Francisco Pintado Fe, n. 26, 33011 Oviedo, Spain

ABSTRACT: The characterization of the segregation phenomena in binary mixtures of solids with very different densities and/or particle sizes is highly relevant in many industrial processes. As a recent example, some advanced CO_2 capture systems using fluidized beds include the separation by segregation of the functional materials. In this work, we have conducted mixing-segregation experiments with particles of iron ore (a typical oxygen carrier in chemical looping combustion systems) acting as jetsam, and glass beads (representing a lower density solid present in the bed) acting as flotsam, to measure solid concentration profiles at different fluidizing gas velocities and mixture compositions of different-sized particles. The experimental concentration profiles have been interpreted using a modified version of the model proposed by Gibilaro and Rowe. A relatively simple correlation is included in the model to calculate the segregation model parameters, which depend on the physical properties of the fluidized solids. The model fits reasonably well with all experimental data, especially for mixtures with a low fraction of oxygen carriers, which are the most relevant for the design of future continuous separation of solids by segregation.

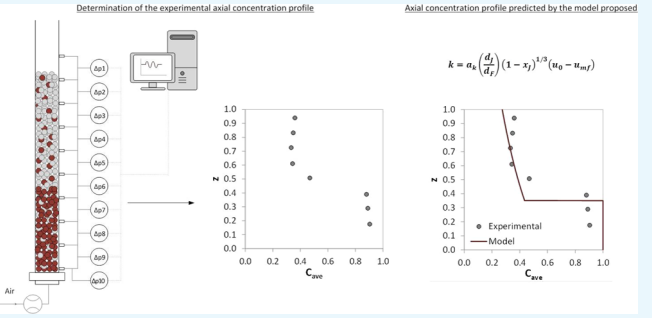

INTRODUCTION

Fluidized beds containing mixtures of solids with different particle size and/or density are commonly used in industrial processes. In many cases, distinct degrees of mixing or segregation are required.[1−4] This paper is motivated by recent proposals in the emerging field of high-temperature solid looping cycles for CO_2 capture, which include a continuous separation step of dense solids.[5−14] The targeted separation is usually between oxygen carrier particles containing a transition metal and lighter solids in the bed: usually, a porous CO_2 sorbent material containing CaO or unconverted solid fuel particles. In systems involving calcination of $CaCO_3$, a large flow of dense solids oxidized in the air reactor transports as sensitive heat at very high temperatures, the energy needed for the regeneration of the CO_2 sorbents.[8,9,11,14] However, once the CO_2 sorbent is regenerated, a sufficient separation of the oxygen carrier from the lighter sorbent particles is required. In a process under development by General Electric, Jayarathna et al.[11] achieved this solid separation in experiments carried out in an entrainment bed. Other authors have proposed the use of bubbling beds to favor the solid segregation in this type of systems.[6,8,9,15−19]

The prediction of the behavior and fluid dynamics of binary mixtures is complex and the separation efficiency attainable by segregation is highly uncertain. It is generally accepted[20−27] that the action of bubbles in fluidized beds produces mixing of the solid components, as well as low gas velocities, and different physical properties between the solids of a mixture lead to the segregation of the particles along the bed height. The lighter and/or smaller-sized component will tend to accumulate at the top of the bed (flotsam) and the heavier and/or larger-sized component will sink to the bottom (jetsam). Mixing and segregation compete during fluidization causing the mobility of the solids until a certain equilibrium distribution is achieved.[1,20,28−33] Numerous investigations to quantify where and how this equilibrium is reached have been reported in the literature. Some researchers have been dedicated to study the influence of the solid properties on the axial solid concentration profiles resulting from segregation,[30,34,35] to formulate indexes that quantify the degree of mixing during fluidization[23,36−38] or to predict the segregation direction.[39,40] However, most of the early studies on segregation were extremely sensitive to the particular characteristics of the solids and the experimental setup, as no model was available to generalize the observations.

Gibilaro and Rowe[20] first proposed a two-phase model (GR model) to describe segregating fluidized beds, in which the bed is assumed to be composed of the wake phase (i.e., the fraction of solids ascending with the bubbles) and of the bulk phase (i.e., the rest of the solids in the bed). Three mechanisms of mixing (circulation, exchange and axial mixing) and one of segregation, represented by their corresponding parameters, are considered in the model. With the circulation mechanism, the bubbles sweep along solids from the bottom of the bed to the top. Then, the solids abandon the wake phase to join the bulk and flow down. Moreover, there is a continuous exchange of solids between the bulk and wake phases along the bed. Finally,

Received: March 11, 2019
Accepted: May 13, 2019
Published: May 23, 2019

DOI: 10.1021/acsomega.9b00674
ACS Omega 2019, 4, 9065−9073

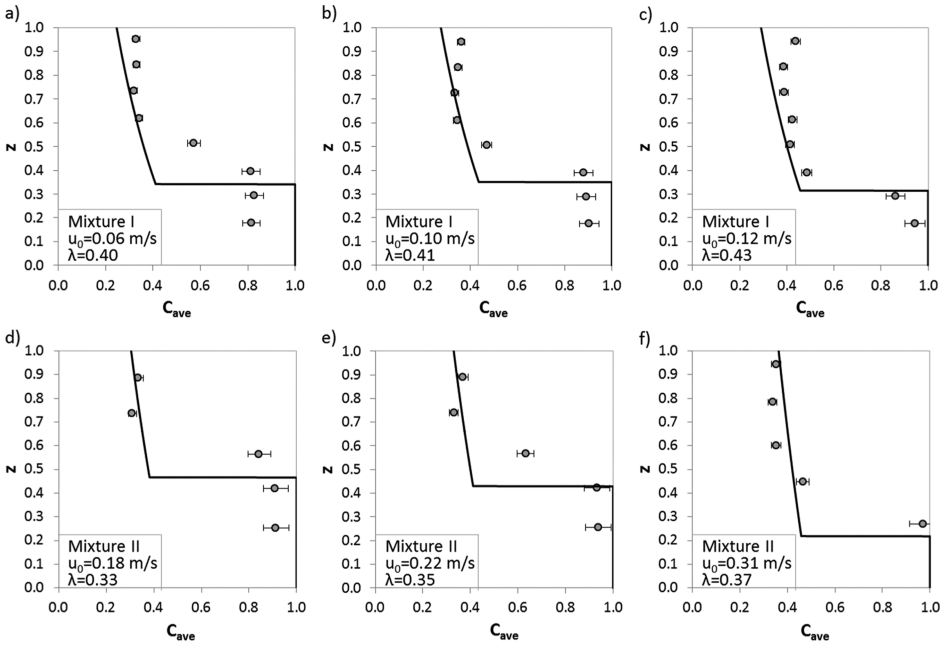

Figure 1. Effect of gas fluidizing velocity on segregation of mixture I (a–c) and mixture II (d–f). Both mixtures contained a mass fraction of jetsam of 0.7. Solid lines correspond to model predictions for $a_k = 1/3$.

bubble movement causes axial mixing in the bulk phase, giving rise to solid dispersion in the vertical direction that can be described as a diffusion process. The segregation mechanism depends not only on the flow of bubbles, but also on the difference in physical properties of the solids (mainly density and size).[1,20] Hence, during the fluidization of a binary mixture that contains solids of similar characteristics, the particles will tend to be uniformly arranged along the bed. In contrast, when the solids greatly differ in density and/or particle size, two clearly differenced zones will appear, that is, a pure-jetsam region settled at the bottom of the bed and an upper zone where the predominant component is the flotsam. Both zones are separated at a critical height.[20] In an intermediate scenario, there will not be a pure-jetsam zone at the bottom and a gradient of jetsam will be observed along the bed. These concepts have been used in subsequent works to describe segregation phenomena in numerous binary systems. Naimer et al.[31] proposed correlations for the calculation of the GR model parameters based on the properties of the bubbles and the solids and solved the differential equations for jetsam-poor mixtures. Hoffmann et al.[22] extended the use of the previous methodology to jetsam-rich and equal-density mixtures by redefining some correlations. Bilbao et al.[41] described in detail the segregation of a mixture of straw and sand by modifying the GR model accounting for the peculiar physical characteristics of straw. García-Ochoa et al.[42] focused their research on binary mixtures of solids of group D according to Geldart's classification.[43] The values of the parameters of the GR model were directly obtained from the fitting of the experimental results instead of using correlations that depend on the operating conditions. Abanades et al.[44] adapted the GR model to explain the segregation during fluidization of mixtures of limestone and coal operating in slugging regime. They observed that the circulation of solids depends on the oscillations caused by the gas slugs and the particles are segregated following a simple mechanism of free falling. In a more recent work, Kumar et al.[45] combined an adapted version of the GR model with a pressure gradient model in order to describe segregation in gas–solid vacuum-fluidized beds.

Apart from the models, based on the GR model, other methodologies have been developed to quantify the segregation phenomena in fluidized beds. Tanimoto et al.[46] investigated the descending motion of different jetsams and calculated their downward velocity by means of a model with no adjustable parameters, which is especially suitable for mixtures of solids with similar minimum fluidization velocity. Chen[47] developed a theoretical model only applicable for solid mixtures of the same density, in which the bed is divided into a static phase at the bottom and a well-mixed fluidized phase above the static phase. The segregation is characterized by means of the initial solid concentration profile and the physical properties of gas and particles. Burgess et al.,[48] Yoshida et al.[49] and Gelperin et al.[50] suggested different models based on nondeterministic parameters (i.e., independent of the operating conditions), which are difficult to relate to the behavior of the solids mixture. Burgess et al.[48] proposed a numerical model, in which the bubble wake is assumed to be composed of both unmixed and mixed fractions exchanging solids with the emulsion phase. Yoshida et al.[49] developed a model only valid for mixtures of solids with the same density, assuming that solid segregation is due to different exchange rates of particles between the wake and bulk phases. Gelperin et al.[50] proposed a two-parameter empirical model based on the mechanisms of segregation and axial dispersion and only valid for equal-density mixtures. Finally, Girimonte et al.[51,52] have recently developed a simple fundamental model to predict the axial solid concentration profile from the fluidization velocity diagram by relating the fluidization to the extent of segregation. This relationship is independent of the effect of bubbling. The fluidization of binary mixtures has been also studied using computational fluid dynamics.[6,27,53−59] Its use has increased in the last two decades because of the improvements in computational power and the increasing reliability of the codes when modeling dense fluidized bed systems. These techniques have already

DOI: 10.1021/acsomega.9b00674
ACS Omega 2019, 4, 9065−9073

demonstrated their capability to obtain relevant information on the segregation mechanism. However, their practical application to a wide range of solid shape and size relevant in specific application is not straightforward, and empirical approaches combined with semimechanistic models of the segregating solid phases in the bed are still useful.

In this work, mixing-segregation experiments have been conducted to investigate the segregation behavior of an iron oxide, which is a typical oxygen carrier used in chemical looping combustion applications.[60−68] The GR model framework has been adopted to interpret the observed experimental results, showing a reasonable accuracy to capture the main trends observed in the tests once the model parameters are tuned to incorporate specific solid particle properties.

RESULTS AND DISCUSSION

The effects of the fluidizing gas velocity, the mass fraction of jetsam, and the particle size of the jetsam on solid segregation pattern have been analyzed in detail for the binary mixtures listed in Table 2. In order to facilitate the understanding of the results, the dimensionless number λ that relates the circulation rate (w) with the segregation rate (k) has been used as an indicator of the segregation tendency of the solids mixture.[20,31] Thus, higher values of λ denote a lower tendency to segregate (i.e., higher values of solid circulation rates and reduced segregation rates) and vice versa.

Figure 1 shows the axial concentration profiles for both mixtures I and II containing a mass fraction of jetsam of 0.7 at increasing fluidizing gas velocities of up to 0.31 m/s. As can be seen, the increase in gas velocity in both fluidized mixtures results in a better mixing of the solids. The critical height (z^*) that separates the zones enriched in jetsam and flotsam is slightly reduced and the concentration of jetsam in the upper region of the bed increases at higher gas velocities.

Moreover, the values calculated for λ demonstrate that mixture II (containing larger particles of iron oxide) exhibits greater tendency to segregate. Lower values of λ were obtained for mixture II (around 0.35 vs 0.40 for mixture I) in tests carried out at three times higher gas velocities. As can be seen, the weight fractions of jetsam in every condition tested are reasonably well predicted by the model assuming a value of 1/3 for the adjustable parameter a_k included in eq 17.

In Figure 2a, the linear dependency of the segregation rate (k) with the gas velocity (eq 17) is represented for both solid mixtures. As expected, higher values of k are obtained for mixture II, which contains larges particles of iron oxide. When operating with a fraction of jetsam of 0.3 and around 0.1 m/s of inlet gas, a value of k of about 0.10 is obtained for mixture II. However, a significantly lower value for k of about 0.06 is calculated in the same conditions for mixture I. The effect of the gas velocity on the solid circulation rate (w) is more moderate. As can be seen in Figure 2b, a modest increase in λ is obtained at growing gas flowrates in both mixtures. Moreover, higher fractions of jetsam favor the mixing of the solids bed, giving rise to values for λ above 0.70 for both mixtures in the whole range of gas velocities tested.

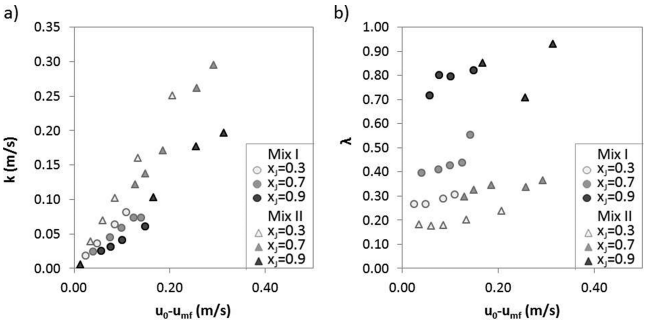

Figure 2. (a) Evolution of the parameter λ with the fluidizing gas velocity. (b) Evolution of the segregation rate (eq 16) with the fluidizing gas velocity. The fluidizing gas velocity ranged from 0.04 to 0.42 m/s.

Figure 3 illustrates the effect of the jetsam concentration in the experimental and predicted solid segregation profiles

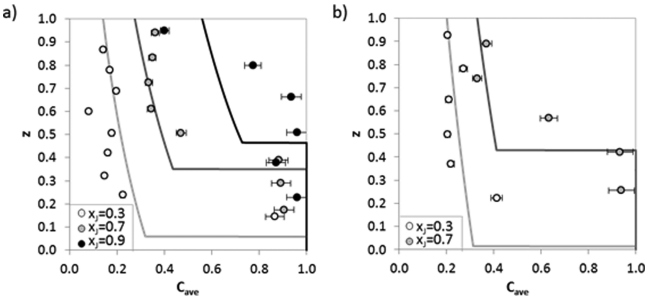

Figure 3. Effect of the mass fraction of jetsam on the segregation: (a) mixture I; u_0 = 0.10 m/s; $\lambda_{(x_j=0.3)}$ = 0.29, $\lambda_{(x_j=0.7)}$ = 0.41, $\lambda_{(x_j=0.9)}$ = 0.72. (b) Mixture II; u_0 = 0.22 m/s; $\lambda_{(x_j=0.3)}$ = 0.24, $\lambda_{(x_j=0.7)}$ = 0.35. Solid lines correspond to model predictions for a_k = 1/3.

obtained at a constant fluidizing gas velocity. A rise in x_J increases the tendency to solid mixing. As a consequence of a higher proportion of jetsam in the fluidized bed, the critical height (z^*) that separates the almost pure jetsam zone located at the bottom from the upper region enriched in jetsam is increased. Moreover, greater concentrations of jetsam above z^* are observed at higher x_J and the segregation profiles are gradually less pronounced.

This trend is confirmed in Figure 4, in which the evolution of the parameter λ with the mass fraction of jetsam is represented.

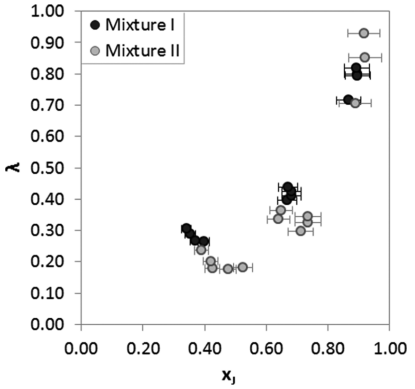

Figure 4. Evolution of the parameter λ with the mass fraction of jetsam.

Mixing gains importance with respect to segregation in mixtures containing about 0.9 fraction of jetsam, giving rise to calculated values of λ between 0.7 and 0.92. In contrast, in mixtures with lower amount of jetsam (x_J < 0.55), the segregation phenomenon clearly prevails and values of λ of below 0.3 are obtained.

DOI: 10.1021/acsomega.9b00674
ACS Omega 2019, 4, 9065−9073

The effect of the particle size of the denser solid on the segregation profiles at two different gas velocities is represented in Figure 5 (maintaining a constant x_J of 0.3 in the tests). As can

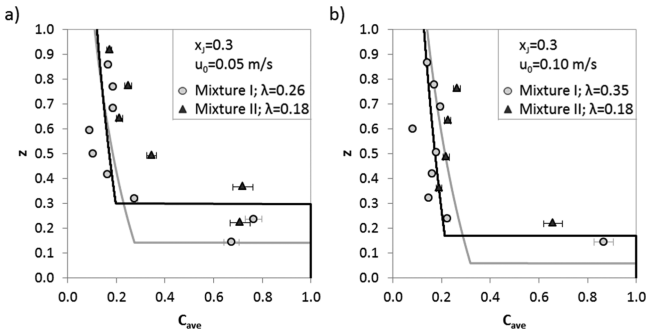

Figure 5. Influence of the particle size of the denser solid in the segregation profiles. Test conditions for both mixtures: (a) x_J = 0.3; u_0 = 0.05 m/s; (b) x_J = 0.3; u_0 = 0.10 m/s. Solid lines correspond to model predictions for a_k = 1/3.

be seen in Table 2, the mixture II that contains larger particles sizes of iron oxide (i.e., of between 355 and 400 μm vs 200−250 μm of mixture I) exhibits a much higher ratio of minimum fluidization velocities of its components (u_p/u_f = 28). During the fluidization of mixture II, the zone of the bed enriched in jetsam is expanded and the critical height z^* is located above that observed during the fluidization of the mixture I, regardless of the inlet gas velocity. The values of λ obtained for mixture II are significantly lower and they are less affected by growing gas velocities, which demonstrates a greater tendency to segregate of this solids mixture.

In Figure 6, the average volumetric fractions of jetsam obtained at the different experimental conditions are compared

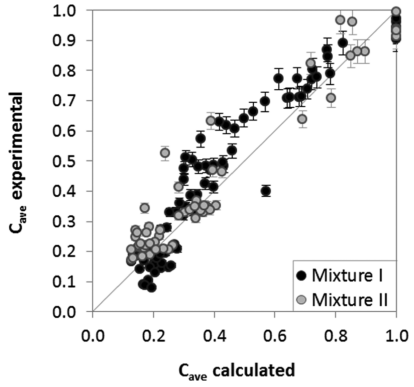

Figure 6. Comparison between the experimental average volumetric fractions of jetsam and the calculated values according to the model proposed with a_k = 1/3. Tests were carried out with u_0 ranging from 0.04 to 0.42 and x_J from 0.3 to 0.9.

with the concentrations predicted by the model assuming a value of 1/3 for the adjustable parameter a_k (eq 17). As can be seen, the model gives a satisfactory prediction of jetsam concentration, especially for the experiments carried out with mixture II containing a C_{ave} of below 0.5. However, the model tends to underpredict the values of the average volumetric fractions of jetsam for experiments with mixture I containing C_{ave} higher than 0.3.

As explained above, several authors[74−76] have calculated the segregation rate coefficient (k) proposed by Naimer et al.[31] (eq 8) on the basis of different formulations for the dimensionless segregation distance ($\overline{Y}_s$), which depends not only on the physical properties of the solids but also on the fluid dynamics of the bed (eqs 14−16).

Figure 7 compares the quality of the fit of different correlations reported in the literature with the equation proposed in this work. As can be seen, the correlations proposed by Hoffmann and Romp.[75] and Dechsiri et al.[76] (eqs 15 and 16, respectively) describe accurately the segregation profiles of mixtures with low concentrations of jetsam (Figure 8a,c). However, both equations fail when predicting segregation patterns of high jetsam concentration mixtures (Figure 7b,d). Better results are obtained with the model based on the dimensionless segregation distance proposed by Tanimoto et al.,[74] but considerable deviations from the experimental data are still observed. With respect to the correlation proposed in this work, the segregation profiles are more accurately described in general, especially for mixtures with low fractions of jetsam.

These results demonstrate that the proposed model, which is based on parameters relatively easy to estimate, is able to predict the segregation patterns of binary mixtures with solids differing sufficiently in their physical properties, regardless of the velocity of the fluidizing gas and the mass fraction of jetsam in the mixture.

CONCLUSIONS

A model based on that reported by Gibilaro and Rowe[20] has been proposed to describe the segregation of solids with very different physical properties during fluidization. Apart from the segregation phenomenon, the solid circulation from the bottom to the top of the fluidized bed (and vice versa), and the exchange of solids between the wake and bulk phases determine the distribution of the flotsam and jetsam during fluidization. However, the influence of the axial mixing in the bulk phase to the mixing process is assumed to be negligible in view of the experimental results. A relatively simple correlation to calculate the segregation rate, which only depends on the physical properties of the fluidized solids, has been included in the model. The fluidization of two different binary mixtures containing glass spheres of 70−110 μm and iron oxide particles of 200−250 and 355−400 μm, respectively, has been studied. Mass fractions of jetsam from 0.3 to 0.9 have been tested in both mixtures using fluidizing gas velocities ranging between 0.04 and 0.42 m/s. It has been observed that higher fluidizing gas velocities favor the mixing of the solids. A raise in the proportion of jetsam also increases the tendency to the solid mixing, giving rise to less-pronounced segregation profiles. In contrast, larger particle sizes of jetsam result in stronger solid segregation. The model developed in this work is able to describe accurately the solid concentration profiles in every condition tested, especially in the tests carried out with relatively low proportion of jetsam. A comparison with other segregation models available in the literature has demonstrated that the proposed model describes better the segregation profiles of this kind of solids mixtures in a wider range of operating conditions.

METHODOLOGY

The experiments to study the segregation of binary mixtures during fluidization were carried out at room temperature and at atmospheric pressure using a 1 m high methacrylate column with an inner diameter of 42 mm (see Figure 1a). Ten pressure

DOI: 10.1021/acsomega.9b00674
ACS Omega 2019, 4, 9065−9073

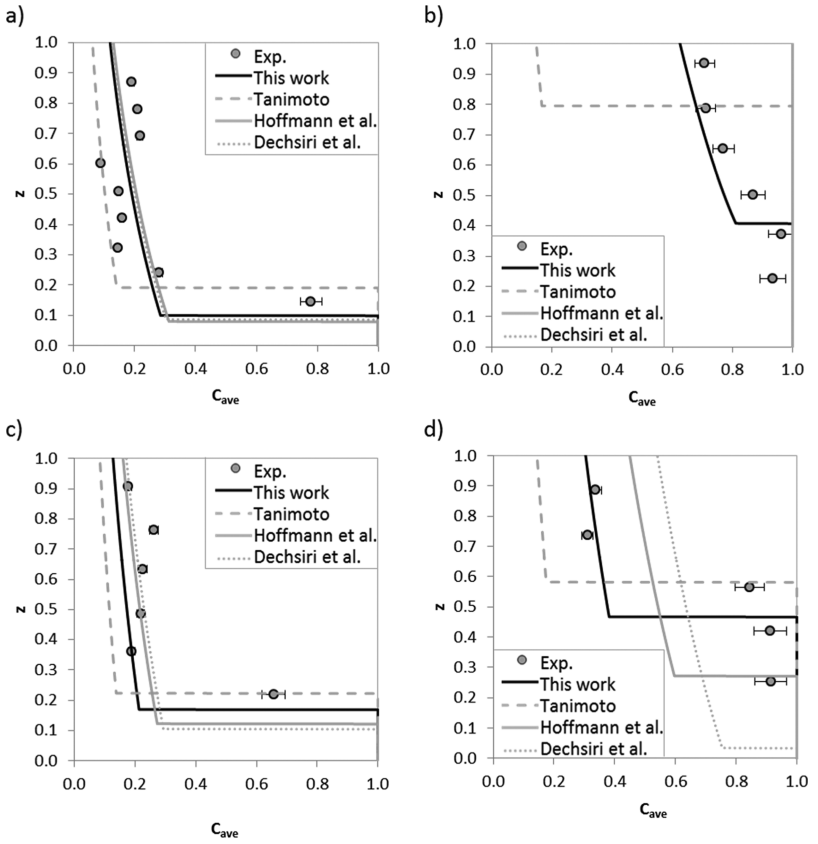

Figure 7. Comparison between the predictions of the experimental axial concentration profiles according to the model proposed and those obtained from other models reported in the literature.[74−76] Experimental conditions: (a) mixture I, $x_J = 0.3$, $u_0 = 0.06$ m/s; (b) mixture I, $x_J = 0.9$, $u_0 = 0.12$ m/s; (c) mixture II, $x_J = 0.3$, $u_0 = 0.10$ m/s; (d) mixture II, $x_J = 0.7$, $u_0 = 0.18$ m/s.

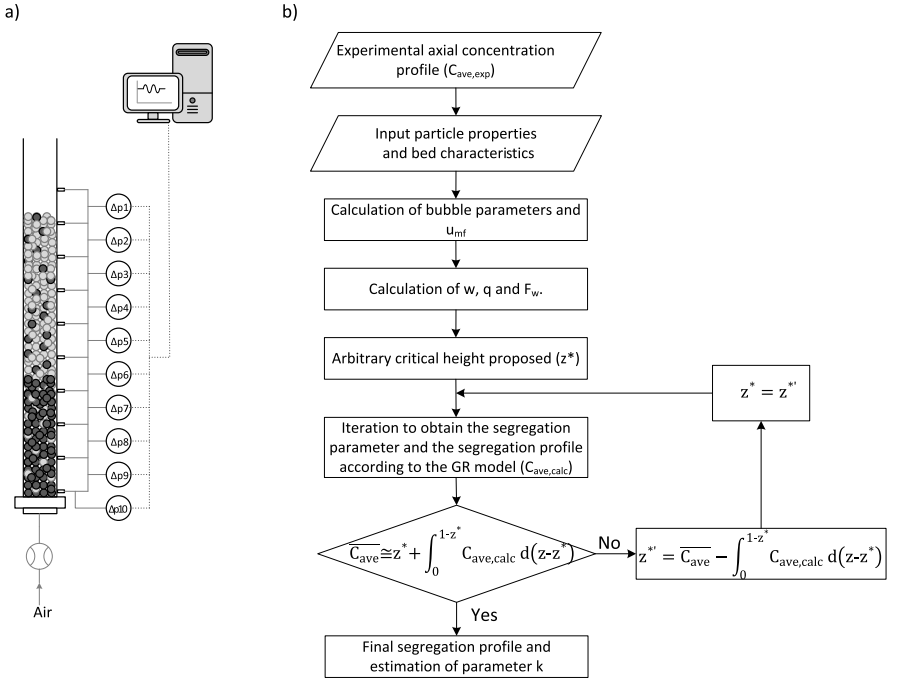

Figure 8. (a) Scheme of the experimental setup; (b) iterative procedure for the calculation of the segregation parameter k according to the GR model.

taps separated 30 mm each other along the column allowed the measurement of nine ΔP at different heights. The electric signals generated by the pressure sensors were registered in a computer using a data logger. Air, regulated by a mass flow controller, was used as fluidizing gas. A perforated plate was used as the distributor of the air in the fluidized bed. A gas flow

DOI: 10.1021/acsomega.9b00674
ACS Omega 2019, 4, 9065−9073

rate between 3 and 35 Nl/min was fed into the column depending on the test. Iron oxide particles of between 200 and 400 μm obtained after crushing and sieving solids of mineral ore were mixed in different proportions (from 30 to 90% wt) with glass spheres with particle diameters of between 70 and 110 μm. Amounts of solids from 350 to 750 g were loaded in the column depending on the experiment. The main characteristics of the solids used in this work are detailed in Table 1.

Table 1. Main Properties of the Solids Used in the Experimental Campaign

solid	Geldart group[43]	d (μm)	ρ (kg/m^3)	u_{mf} (m/s)
iron oxide	B	355−400	4600	0.229
iron oxide	B	200−250	4600	0.075
glass spheres	A	70−110	2500	0.008

In a typical experiment, a mixture of solids with known concentration is exposed to strong fluidization (i.e., gas velocities of between 0.3 and 0.6 m/s) for 5−10 min. Then, the flow of inlet gas is cutoff, thereby obtaining a perfectly mixed-solid bed. Later, the bed is subjected to fluidization at a gas velocity above the minimum fluidization velocity (u_{mf}) of the component with higher u_{mf} (typically the jetsam, although this is not always the case[30]) in order to induce the segregation of the components. The flow of air should be kept constant until an equilibrium distribution of the solids is achieved. In that moment, the air flow is cutoff again in order to freeze the bed, so that the axial concentration profile can be determined following the procedure developed in a previous work.[69]

The proposed methodology basically consists in calculating the minimum fluidization velocity from pressure drop measurements at different inlet gas velocities.[70,71] For this purpose, the pressure drops measured at different heights of the bed are recorded at increasing gas velocities and after that, the minimum fluidization velocity can be easily derived from the Ergun equation.[70] These gas velocities should be sufficiently low to avoid any alteration of the solids concentration profile. Finally, the concentration of jetsam at each bed slice is obtained from the u_{mf} measured,[72] by applying the correlation developed by Turrado et al.,[69] which relates the minimum fluidization of the mixture measured at a certain slice of the bed with the mass fraction of jetsam present there (x_p) and the minimum fluidization velocity of the pure components (u_p and u_f), by means of a mixture-dependent parameter

$$u_{mf} = u_f \left(\frac{u_p}{u_f}\right)^{x_p^{\,b}} \tag{1}$$

This correlation is particularly appropriate for mixtures of solids with very different u_{mf} as the two binary mixtures (I and II, as indicated in Table 2) investigated in this work (mixture I: $b = 1.88 + 0.79x_p$; mixture II: $b = 3.02$).[69] Mixture I and mixture II contain glass spheres of 70−110 μm combined with iron oxide particles of 200−250 and 355−400 μm, respectively. Mass fractions of jetsam (x_J) from 0.3 to 0.9 were tested with both mixtures using fluidizing gas velocities ranging between 0.04 and 0.42 m/s.

Mathematical Model. A modification of the GR model[20] was used to provide an interpretation for the segregation patterns observed experimentally in this work. The GR model considers three mechanisms responsible for mixing and one for segregation. Each mechanism is represented by a parameter: w, q, r, and k, which are the solid circulation rate, the exchange rate, the axial mixing rate, and segregation rate, respectively. The influence of the axial mixing in the bulk phase to the mixing process was assumed to be negligible (i.e., the case 2 of the GR model[20]) as any experimental evidence of this phenomenon was observed during the tests.[31,46] In the GR model, it is assumed that neither mixing nor segregation occurs in the horizontal plane and that w, q, and k are independent of the bed height. Furthermore, different packing densities along the bed and the space occupied by the bubbles were ignored when considering elementary volumes of the bed. Therefore, the following differential equations, that describe the jetsam movement in the bulk and in wake phase, are obtained when solving the balance to an elementary slice of the bed of thickness dz[20]

$$\frac{dC_B}{dz}(w + k - 2kC_B) + qH(C_w - C_B) = 0 \tag{2}$$

$$w\frac{dC_w}{dz} - qH(C_B - C_w) = 0 \tag{3}$$

where C_B and C_W are the volumetric fraction of jetsam in the bulk and wake phase, respectively, z is the normalized height and H the total bed height. The average jetsam concentration in the bed (C_{ave}) can be calculated from the fraction of solids in the wake phase (F_w) as follows

$$C_{ave} = F_w C_W - (1 - F_w)C_B \tag{4}$$

The parameters F_w, w, q, and k can be obtained from the correlations proposed by Naimer et al.[31]

$$F_W = \frac{a_B' F_{WB}}{1 - a_B} \tag{5}$$

$$w = u_b F_{WB}\left(\frac{a_B'}{1 - a_B'}\right) \tag{6}$$

$$q = 1.5\frac{F_{WB}u_{mf}}{d_B \epsilon_{mf}}\left(\frac{a_B'}{1 - a_B'}\right) \tag{7}$$

Table 2. Main Characteristics of the Solids Mixtures and Operating Conditions during Fluidization Tests

mixture	jetsam	flotsam	u_p/u_f	x_J	u_0 range (m/s)
I	iron oxide (200−250 μm)	glass spheres (70−110 μm)	9.38	0.3	0.04−0.12
				0.7	0.06−0.17
				0.9	0.06−0.19
II	iron oxide (355−400 μm)	glass spheres (70−110 μm)	28.63	0.3	0.05−0.22
				0.7	0.12−0.31
				0.9	0.21−0.42

DOI: 10.1021/acsomega.9b00674
ACS Omega 2019, 4, 9065−9073

$$k = \frac{3}{4}\overline{Y}_s u_b \left(\frac{a'_B}{1 - a'_B}\right) \quad (8)$$

where a'_B is the volume fraction of wakes and bubbles in the bed, F_{WB} is the volume fraction of the wake in the bubble, a_B is the volume fraction of bubbles in the bed, u_b is the bubble rise velocity, d_b is the bubble diameter, ϵ_{mf} is the bed voidage at minimum fluidization velocity, and $\overline{Y}_s$ is the dimensionless segregation distance. The equations taken from literature for their calculation are listed in Table 3.

Table 3. Equations for the Calculation of Fluidization Parameters Included in the Model

Bubble rise velocity[73]

$$u_b = (u_0 - u_{mf}) + 0.711\sqrt{g d_b} \quad (9)$$

volume fraction of the wake in the bubble[31]

$$F_{WB} = \frac{1}{2} - \frac{9}{16}\cos\left(\frac{\theta_W}{2}\right) + \frac{1}{16}\cos\left(\frac{3\theta_W}{2}\right) \quad (10)$$

wake angle[22]

$$\theta_W = 160 - 160\, e^{(-60 d_b)} \quad (11)$$

volume fraction of wakes and bubbles in the bed[31]

$$a'_B = \frac{u_0 - u_{mf}}{u_b(1 - F_{WB})} \quad (12)$$

volume fraction of bubbles in the bed[31]

$$a_B = (1 - F_{WB})a'_B \quad (13)$$

dimensionless segregation distance[74−76]

$$\overline{Y}_s = 0.6\left(\frac{\rho_J}{\rho_F}\right)\left(\frac{d_J}{d_F}\right)^{1/3} \quad (14)$$

$$\overline{Y}_s = 0.8\left(\frac{\rho_J}{\rho_{bulk}}\right)\left(\frac{d_J}{d_{bulk}}\right)^{1/3} - 0.8 \quad (15)$$

$$\overline{Y}_s = 0.8\left[\frac{d_J \rho_J^{1/3}}{(1 - \overline{C_{ave}})\rho_F d_F^{1/3} + \overline{C_{ave}}\rho_J d_J^{1/3}} - 1\right] \quad (16)$$

According to Naimer et al.,[31] the segregation rate coefficient k, which represents the net downward flow of the jetsam compared to the ascending flotsam, is great affected by the fluid dynamics of the bed (eq 8). However, during the experimental campaigns solid segregation was observed to depend basically on the physical properties of the fluidized solids. The segregation rate coefficient k was calculated as an adjustable parameter to find the most accurate description of the experimental results. The value of k obtained for each condition depended on the fluidizing gas velocity, the minimum fluidization velocity of the mixture, the particle sizes, and bed composition. According to that, the following correlation to determine the segregation coefficient rate was formulated

$$k = a_k\left(\frac{d_J}{d_F}\right)(1 - x_J)^{1/3}(u_0 - u_{mf}) \quad (17)$$

where a_k is an adjustable parameter, d_J and d_F are the particle diameter of the jetsam and flotsam, respectively, x_J is the mass fraction of jetsam, u_0 the fluidizing gas velocity and u_{mf} the minimum fluidization velocity of the mixture for that specific mass fraction of jetsam.

During the experiments, it was observed that most of the solids located above the critical height z^* (whose value varied depending on the fluidization conditions) were flotsam. Hence, it was assumed for the calculations that the properties of the solids located in that part of the column were inalterable and corresponded to the flotsam. Moreover, the bubble size was considered to be about half of the column diameter (i.e., 21 mm) and remained stable during the upward movement, in the same way that other fluid−dynamic parameters, such as the bubble rise velocity (u_b), the volume fraction of the wake in the bubble (F_{WB}), the volume fraction of solids in the wake (F_w) and the coefficients of segregation (k), exchange (q), and circulation (w).

The methodology followed in this work to solve the differential equations and then obtain the critical height and the segregation constant (k) that better describes the experimental results is represented in Figure 8b. The bubble properties were first estimated by means of eqs 9−13, which allowed the fraction of solids in the wake phase (F_w) and the parameters of exchange and circulation (q and w, respectively) to be obtained (eqs 5−7). Because the value of z^* cannot be directly derived from the experimental data, an iterative procedure was followed to obtain both the critical height (z^*) and segregation rate (k). Thus, an arbitrary critical height (z^*) was initially assumed and a value of the parameter k was obtained by applying least-squares fitting to the experimental curves. If the supposed values of z^* and k fulfilled the mass balance represented by eq 18, they could be considered valid. If not, the value obtained for the arbitrary critical height ($z^{*\prime}$) that closed the mass balance was used in the following iteration, thereby calculating the corresponding new value of k.

$$\overline{C_{ave}} = z^* + \int_0^{1-z^*} C_{ave,calc}\, d(z - z^*) \quad (18)$$

This procedure was successively repeated until the convergence was achieved. Once the segregation coefficient rates (k) were estimated for every solids mixture and fluidizing conditions tested, the adjustable parameter a_k, that relates the segregation rate with gas velocity and solid bed properties (eq 17), was calculated by least-squares method.

AUTHOR INFORMATION

Corresponding Author

*E-mail: jramon@incar.csic.es. Phone: +34 985 11 90 90.

ORCID

José Ramón Fernández: 0000-0001-9801-7043

Notes

The authors declare no competing financial interest.

ACKNOWLEDGMENTS

The authors acknowledge the financial support received from the Spanish Ministry of Economy, Industry and Competitivity (ENE2015-68885-C2-1-R).

LIST OF SYMBOLS

a'_B, volume fraction of wakes and bubbles in the bed (-)
a_k, coefficient of the correlation for the segregation parameter (-)
b, adjustable parameter of Turrado et al.[69] equation (-)
C_{ave}, average volumetric fraction of jetsam from both bulk and wake phases (-)
$\overline{C_{ave}}$, average volumetric fraction of jetsam from both bulk and wake phases in the whole bed (-)
C_B, volumetric fraction of jetsam in the bulk phase (-)

DOI: 10.1021/acsomega.9b00674
ACS Omega 2019, 4, 9065−9073

C_W, volumetric fraction of jetsam in the wake phase (-)
d, particle diameter (m)
d_b, bubble diameter (m)
F_w, volume fraction of solid in the wake (-)
F_{WB}, volume fraction of the wake in the bubble (-)
H, total bed height (m)
k, segregation coefficient (m/s)
q, exchange rate coefficient (s^{-1})
u, velocity (m/s)
w, solids circulation rate (m/s)
x_J, mass fraction of the jetsam (-)
$\overline{Y}_s$, dimensionless segregation distance (-)
z, normalised height (-)
z^*, normalised critical height (-)

GREEK LETTERS

Δp, bed pressure drop (Pa)
ϵ, bed voidage (-)
ρ, density (kg/m^3)

SUBSCRIPT

0, fluidizing gas
b, bubble
bulk, bulk
f, component with the lowest minimum fluidization velocity
F, flotsam
J, jetsam
mf, minimum fluidization conditions of the mixture
p, component with the highest minimum fluidization velocity

REFERENCES

(1) Rowe, P. N.; Nienow, A. W. Particle mixing and segregation in gas fluidised beds. A review. *Powder Technol.* **1976**, *15*, 141−147.
(2) Kunii, D.; Levenspiel, O.; Brenner, H. *Fluidization Engineering*; Elsevier Science, 1991.
(3) Leckner, B. Fluidized bed combustion: Mixing and pollutant limitation. *Prog. Energy Combust. Sci.* **1998**, *24*, 31−61.
(4) Wall, T. F. Combustion processes for carbon capture. *Proc. Combust. Inst.* **2007**, *31*, 31−47.
(5) Alghamdi, Y. A.; Doroodchi, E.; Moghtaderi, B. Mixing and segregation of binary oxygen carrier mixtures in a cold flow model of a chemical looping combustor. *Chem. Eng. J.* **2013**, *223*, 772−784.
(6) Peng, Z.; Doroodchi, E.; Alghamdi, Y.; Moghtaderi, B. Mixing and segregation of solid mixtures in bubbling fluidized beds under conditions pertinent to the fuel reactor of a chemical looping system. *Powder Technol.* **2013**, *235*, 823−837.
(7) Bao, J.; Li, Z.; Cai, N. Experiments of char particle segregation effect on the gas conversion behavior in the fuel reactor for chemical looping combustion. *Appl. Energy* **2014**, *113*, 1874−1882.
(8) Fernández, J. R.; Abanades, J. C. CO2 capture from the calcination of CaCO3 using iron oxide as heat carrier. *J. Cleaner Prod.* **2016**, *112*, 1211−1217.
(9) Fernández, J. R.; Abanades, J. C. Sorption enhanced reforming of methane combined with an iron oxide chemical loop for the production of hydrogen with CO2 capture: Conceptual design and operation strategy. *Appl. Therm. Eng.* **2017**, *125*, 811−822.
(10) Kraft, S.; Kirnbauer, F.; Hofbauer, H. Investigations using a cold flow model of char mixing in the gasification reactor of a dual fluidized bed gasification plant. *Powder Technol.* **2017**, *316*, 687−696.
(11) Jayarathna, C. K.; Chladek, J.; Balfe, M.; Moldestad, B. M. E.; Tokheim, L.-A. Impact of solids loading and mixture composition on the classification efficiency of a novel cross-flow fluidized bed classifier. *Powder Technol.* **2018**, *336*, 30−44.
(12) Martínez, I.; Fernández, J. R.; Abanades, J. C.; Romano, M. C. Integration of a fluidised bed Ca-Cu chemical looping process in a steel mill. *Energy* **2018**, *163*, 570−584.
(13) Wang, S.; Yin, W.; Li, Z.; Yang, X.; Zhang, K. Numerical investigation of chemical looping gasification process using solid fuels for syngas production. *Energy Convers. Manage.* **2018**, *173*, 296−302.
(14) Jayarathna, C. K.; Balfe, M.; Moldestad, B. M. E.; Tokheim, L.-A. Improved multi-stage cross-flow fluidized bed classifier. *Powder Technol.* **2019**, *342*, 621−629.
(15) Li, Z.; Sun, H.; Cheng, M.; Chen, D.; Cai, N. In Separation of Lighter Particles from Heavier Particles in Fluidized Bed for SE Hydrogen Production and CLC, *6th High Temperature Solid Looping Cycles Network Meeting, Milan, 1−2 September; Milan*, 2015.
(16) Sun, H.; Cheng, M.; Chen, D.; Xu, L.; Li, Z.; Cai, N. Experimental Study of a Carbon Stripper in Solid Fuel Chemical Looping Combustion. *Ind. Eng. Chem. Res.* **2015**, *54*, 8743−8753.
(17) Sun, H.; Cheng, M.; Li, Z.; Cai, N. Riser-Based Carbon Stripper for Coal-Fueled Chemical Looping Combustion. *Ind. Eng. Chem. Res.* **2016**, *55*, 2381−2390.
(18) Cheng, M.; Sun, H.; Li, Z.; Cai, N. Annular Carbon Stripper for Chemical-Looping Combustion of Coal. *Ind. Eng. Chem. Res.* **2017**, *56*, 1580−1593.
(19) Ryabov, G. A.; Folomeev, O. M.; Dolgushin, I. A. Study of Conditions of Binary Particle Mixture Motion Applied to Chemical Looping Combustion of Fuel with Carbon Dioxide Capture. *Therm. Eng.* **2018**, *65*, 429−434.
(20) Gibilaro, L. G.; Rowe, P. N. A model for a segregating gas fluidised bed. *Chem. Eng. Sci.* **1974**, *29*, 1403−1412.
(21) Beeckmans, J. M.; Stahl, B. Mixing and segragation kinetics in a strongly segregated gas-fluidized bed. *Powder Technol.* **1987**, *53*, 31−38.
(22) Hoffmann, A. C.; Janssen, L. P. B. M.; Prins, J. Particle segregation in fluidised binary mixtures. *Chem. Eng. Sci.* **1993**, *48*, 1583−1592.
(23) Wu, S. Y.; Baeyens, J. Segregation by size difference in gas fluidized beds. *Powder Technol.* **1998**, *98*, 139−150.
(24) Hoomans, B. P. B.; Kuipers, J. A. M.; van Swaaij, W. P. M. Granular dynamics simulation of segregation phenomena in bubbling gas-fluidised beds. *Powder Technol.* **2000**, *109*, 41−48.
(25) Gilbertson, M. A.; Eames, I. Segregation patterns in gas-fluidized systems. *J. Fluid Mech.* **2001**, *433*, 347−356.
(26) Bokkers, G. A.; van Sint Annaland, M.; Kuipers, J. A. M. Mixing and segregation in a bidisperse gas-solid fluidised bed: a numerical and experimental study. *Powder Technol.* **2004**, *140*, 176−186.
(27) Feng, Y. Q.; Yu, A. B. Microdynamic modelling and analysis of the mixing and segregation of binary mixtures of particles in gas fluidization. *Chem. Eng. Sci.* **2007**, *62*, 256−268.
(28) Rowe, P. N.; Nienow, A. W.; Agbim, A. J. The Mechanisms by which particles segregate in gas fluidised beds—binary systems of near-spherical particles. *Trans. Inst. Chem. Eng.* **1972**, *50*, 310.
(29) Chiba, S.; Chiba, T.; Nienow, A. W.; Kobayashi, H. The minimum fluidisation velocity, bed expansion and pressure-drop profile of binary particle mixtures. *Powder Technol.* **1979**, *22*, 255−269.
(30) Chiba, S.; Nienow, A. W.; Chiba, T.; Kobayashi, H. Fluidised binary mixtures in which the denser component may be flotsam. *Powder Technol.* **1980**, *26*, 1−10.
(31) Naimer, N. S.; Chiba, T.; Nienow, A. W. Parameter estimation for a solids mixing segregation model for gas fluidised beds. *Chem. Eng. Sci.* **1982**, *37*, 1047−1057.
(32) Lim, K. S.; Zhu, J. X.; Grace, J. R. Hydrodynamics of gas-solid fluidization. *Int. J. Multiphase Flow* **1995**, *21*, 141−193.
(33) Olivieri, G.; Marzocchella, A.; Salatino, P. Segregation of fluidized binary mixtures of granular solids. *AlChE J.* **2004**, *50*, 3095−3106.
(34) Geldart, D.; Baeyens, J.; Pope, D. J.; Van De Wijer, P. Segregation in beds of large particles at high velocities. *Powder Technol.* **1981**, *30*, 195−205.
(35) Čársky, M.; Pata, J.; Veselý, V.; Hartman, M. Binary system fluidized bed equilibrium. *Powder Technol.* **1987**, *51*, 237−242.
(36) Nienow, A. W.; Rowe, P. N.; Cheung, L. Y.-L. A quantitative analysis of the mixing of two segregating powders of different density in a gas-fluidised bed. *Powder Technol.* **1978**, *20*, 89−97.

DOI: 10.1021/acsomega.9b00674
ACS Omega 2019, 4, 9065−9073

(37) Rice, R. W.; Brainovich, J. F. Mixing/segregation in two- and three-dimensional fluidized beds: Binary systems of equidensity spherical particles. *AlChE J.* **1986**, *32*, 7−16.
(38) Peeler, J. P. K.; Huang, J. R. Segregation of wide size range particle mixtures in fluidized beds. *Chem. Eng. Sci.* **1989**, *44*, 1113−1119.
(39) Di Maio, F. P.; Di Renzo, A.; Vivacqua, V. A particle segregation model for gas-fluidization of binary mixtures. *Powder Technol.* **2012**, *226*, 180−188.
(40) di Renzo, A.; Di Maio, F. P.; Girimonte, R.; Vivacqua, V. Segregation direction reversal of gas-fluidized biomass/inert mixtures - Experiments based on Particle Segregation Model predictions. *Chem. Eng. J.* **2015**, *262*, 727−736.
(41) Bilbao, R.; Lezaun, J.; Menéndez, M.; Abanades, J. C. Model of mixing-segregation for straw/sand mixtures in fluidized beds. *Powder Technol.* **1988**, *56*, 149−155.
(42) García-Ochoa, F.; Romero, A.; Villar, J. C.; Bello, A. A study of segregation in a gas-solid fluidized bed: Particles of different density. *Powder Technol.* **1989**, *58*, 169−174.
(43) Geldart, D. Types of gas fluidization. *Powder Technol.* **1973**, *7*, 285−292.
(44) Abanades, J. C.; Kelly, S.; Reed, G. P. A mathematical model for segregation of limestone-coal mixtures in slugging fluidised beds. *Chem. Eng. Sci.* **1994**, *49*, 3943−3953.
(45) Kumar, A.; Hodgson, P.; Fabijanic, D.; Gao, W.; Das, S. Analytical model to locate the fluidisation interface in a solid-gas vacuum fluidised bed. *Powder Technol.* **2014**, *266*, 463−474.
(46) Tanimoto, H.; Chiba, S.; Chiba, T.; Kobayashi, H., Mechanism of Solid Segregation in Gas Fluidised Beds. In *Fluidization*; Grace, J. R., Matsen, J. M., Eds.; Springer US: Boston, MA, 1980; pp 381−388.
(47) Chen, J. L.-P. A theoretical model for particle segregation in a fluidized bed due to size difference. *Chem. Eng. Commun.* **1981**, *9*, 303−320.
(48) Burgess, J. M.; Fane, A. G.; Fell, C. J. D. Measurement and Prediction of the Mixing and Segregation of Solids in Gas Fluidised Beds, *Proc. of the 2nd PACHEC*, 1977, Vol. *II*, p. 1405, Denver, U.S.A.
(49) Yoshida, K.; Kameyama, H.; Shimizu, F. Mechanism of Particle Mixing and Segregation in Gas Fluidized Beds. In *Fluidization*; Grace, J. R., Matsen, J. M., Eds.; Springer US: Boston, MA, 1980; pp 389−396.
(50) Gelperin, N.; Zakharenko, V.; Ainshtein, V. Segregation of solid particles in a fluidized bed and the equilibrium distribution. *Theor. Found. Chem. Eng.* **1977**, *11*, 475−481.
(51) Girimonte, R.; Formisani, B.; Vivacqua, V. The relationship between fluidization velocity and segregation in two-component gas fluidized beds: Density- or size-segregating mixtures. *Chem. Eng. J.* **2018**, *335*, 63−73.
(52) Girimonte, R.; Formisani, B.; Vivacqua, V. The concentration profile of two-solid beds after slow defluidization: Model and experiment. *Chem. Eng. J.* **2019**, *359*, 1006−1012.
(53) Feng, Y. Q.; Xu, B. H.; Zhang, S. J.; Yu, A. B.; Zulli, P. Discrete particle simulation of gas fluidization of particle mixtures. *AlChE J.* **2004**, *50*, 1713−1728.
(54) Cooper, S.; Coronella, C. J. CFD simulations of particle mixing in a binary fluidized bed. *Powder Technol.* **2005**, *151*, 27−36.
(55) Deen, N. G.; Van Sint Annaland, M.; Van der Hoef, M. A.; Kuipers, J. A. M. Review of discrete particle modeling of fluidized beds. *Chem. Eng. Sci.* **2007**, *62*, 28−44.
(56) Alavi Shoushtari, N.; Hosseini, S. A.; Soleimani, R. Investigation of segregation of large particles in a pressurized fluidized bed with a high velocity gas: A discrete particle simulation. *Powder Technol.* **2013**, *246*, 398−412.
(57) Zhong, H.; Lan, X.; Gao, J.; Xu, C. Effect of particle frictional sliding during collisions on modeling the hydrodynamics of binary particle mixtures in bubbling fluidized beds. *Powder Technol.* **2014**, *254*, 36−43.
(58) Peng, Z.; Alghamdi, Y. A.; Moghtaderi, B.; Doroodchi, E. CFD-DEM investigation of transition from segregation to mixing of binary solids in gas fluidised beds. *Adv. Powder Technol.* **2016**, *27*, 2342−2353.
(59) Chladek, J.; Jayarathna, C. K.; Moldestad, B. M. E.; Tokheim, L.-A. Fluidized bed classification of particles of different size and density. *Chem. Eng. Sci.* **2018**, *177*, 151−162.
(60) Lyngfelt, A.; Leckner, B.; Mattisson, T. A fluidized-bed combustion process with inherent CO2 separation; application of chemical-looping combustion. *Chem. Eng. Sci.* **2001**, *56*, 3101−3113.
(61) Mattisson, T.; Lyngfelt, A.; Cho, P. The use of iron oxide as an oxygen carrier in chemical-looping combustion of methane with inherent separation of CO2. *Fuel* **2001**, *80*, 1953−1962.
(62) Abad, A.; Mattisson, T.; Lyngfelt, A.; Johansson, M. The use of iron oxide as oxygen carrier in a chemical-looping reactor. *Fuel* **2007**, *86*, 1021−1035.
(63) Xiao, R.; Song, Q.; Song, M.; Lu, Z.; Zhang, S.; Shen, L. Pressurized chemical-looping combustion of coal with an iron ore-based oxygen carrier. *Combust. Flame* **2010**, *157*, 1140−1153.
(64) Gu, H.; Shen, L.; Xiao, J.; Zhang, S.; Song, T. Chemical Looping Combustion of Biomass/Coal with Natural Iron Ore as Oxygen Carrier in a Continuous Reactor. *Energy Fuels* **2011**, *25*, 446−455.
(65) Adanez, J.; Abad, A.; Garcia-Labiano, F.; Gayan, P.; de Diego, L. F. Progress in Chemical-Looping Combustion and Reforming technologies. *Prog. Energy Combust. Sci.* **2012**, *38*, 215−282.
(66) Mendiara, T.; de Diego, L. F.; García-Labiano, F.; Gayán, P.; Abad, A.; Adánez, J. On the use of a highly reactive iron ore in Chemical Looping Combustion of different coals. *Fuel* **2014**, *126*, 239−249.
(67) Tong, A.; Bayham, S.; Kathe, M. V.; Zeng, L.; Luo, S.; Fan, L.-S. Iron-based syngas chemical looping process and coal-direct chemical looping process development at Ohio State University. *Appl. Energy* **2014**, *113*, 1836−1845.
(68) Mendiara, T.; Pérez-Astray, A.; Izquierdo, M. T.; Abad, A.; de Diego, L. F.; García-Labiano, F.; Gayán, P.; Adánez, J. Chemical Looping Combustion of different types of biomass in a 0.5 kW th unit. *Fuel* **2018**, *211*, 868−875.
(69) Turrado, S.; Fernández, J. R.; Abanades, J. C. Determination of the solid concentration in a binary mixture from pressure drop measurements. *Powder Technol.* **2018**, *338*, 608−613.
(70) Ergun, S. *Fluid Flow Through Packed Columns*; Chemical Engineering Progress, 1952; pp 89−94.
(71) Noda, K.; Uchida, S.; Makino, T.; Kamo, H. Minimum fluidization velocity of binary mixture of particles with large size ratio. *Powder Technol.* **1986**, *46*, 149−154.
(72) Cheung, L. Y. L.; Nienow, A. W.; Rowe, P. N. Minimum fluidisation velocity of a binary mixture of different sized particles. *Chem. Eng. Sci.* **1974**, *29*, 1301−1303.
(73) Nicklin, D. J. Two-phase bubble flow. *Chem. Eng. Sci.* **1962**, *17*, 693−702.
(74) Tanimoto, H.; Chiba, S.; Chiba, T.; Kobayashi, H. Jetsam descent induced by a single bubble passage in three-dimensional gas-fluidized beds. *J. Chem. Eng. Jpn.* **1981**, *14*, 273−276.
(75) Hoffmann, A. C.; Romp, E. J. Segregation in a fluidised powder of a continuous size distribution. *Powder Technol.* **1991**, *66*, 119−126.
(76) Dechsiri, C., Bosman, J. C., Dehling, H. G., Hoffmann, A. C.; Hui, G. *Proceedings of International Congress on Particle Technology, (PARTEC2001), Nuremberg*: Nuremberg, 2001.

DOI: 10.1021/acsomega.9b00674
ACS Omega 2019, 4, 9065−9073